Available online at www.sciencedirect.com
SCIENCE DIRECT®
Carbohydrate Research 339 (2004) 967–973
Carbohydrate RESEARCH

Conformational analysis and dynamics of mannobiosides and mannotriosides using Monte Carlo/stochastic dynamics simulations

Anna Bernardi,* Andrea Colombo and Inmaculada Sánchez-Medina

Dipartimento di Chimica Organica e Industriale, Universita' degli Studi di Milano, via Venezian I-21, 20133 Milano, Italy

Received 13 October 2003; accepted 14 November 2003

Abstract—The conformation and dynamics of α-(1 → 2)-mannobioside, α-(1 → 6)-mannobioside, and of the trisaccharide α-Man-(1 → 2)-α-Man-(1 → 6)-α-Man-OMe were studied using Monte Carlo/stochastic dynamics (MC/SD) simulations, the AMBER* force field, and the GB/SA implicit water solvation model. The results are in agreement with available experimental data.

Keywords: Mannose oligosaccharides; Molecular dynamics; Conformational analysis

1. Introduction

Oligomannose oligosaccharides form the cores of the majority of N-linked oligosaccharides from glycoproteins. As a consequence of their biological relevance, oligomannoses have attracted a great deal of attention, and in particular their solution conformation has been studied for many years.[1] As part of a project directed toward the design and synthesis of structural mimics of mannose di- and tri-saccharides, we have performed a detailed conformational analysis and molecular dynamics of α-(1 → 2)-mannobioside α-Man-(1 → 2)-α-Man-OMe **1**, α-(1 → 6)-mannobioside α-Man-(1 → 6)-α-Man-OMe **2**, and of the trisaccharide α-Man-(1 → 2)-α-Man-(1 → 6)-α-Man-OMe **3** using Macromodel (Fig. 1). Our results are reported in this paper and compared to previous calculations and available experimental data.

The conformational studies were conducted in three steps, following a protocol that we have recently validated for the conformational analysis of gangliosides.[2] Thus the analysis began by a stochastic search of conformational space using Monte Carlo/energy minimization (MC/EM). The representative low-energy conformations resulting from the search were used as the starting point for a series of dynamic simulations performed with the highly efficient Still–Guarnieri Monte Carlo/stochastic dynamics (MC/SD) algorithm.[3,4] Compared to the MC/EM results, this step produced dynamic conformational maps for the glycosidic linkages, which did not contain any new significant conformations of the sugar backbone but were optimized with respect to the intramolecular H bonding network. Finally, energy minimization of the conformers stored during the dynamic simulations led to minima, which were lower in energy relative to the results of the MC/EM search, basically due to modifications of the hydrogen bond network. In one case, energy reordering of areas of conformational space relative to the MC/EM results was also observed. In all cases, water solvation was accounted for by the implicit Generalized Born/Surface Area (GB/SA) model[5] and AMBER* was used as the force field.

2. Results

2.1. α-Man-(1 → 2)-α-Man-OMe (1)

The conformation and dynamics of the α-Man-(1 → 2)-α-Man linkage has been studied extensively in the oligomannose oligosaccharide $Man_9GlcNAc_2$, the least processed N-glycan from mature glycoproteins.[1]

* Corresponding author. Tel.: +39-02-50314092; fax: +39-02-503140-72; e-mail: anna.bernardi@unimi.it

0008-6215/$ - see front matter © 2003 Elsevier Ltd. All rights reserved.
doi:10.1016/j.carres.2003.11.013

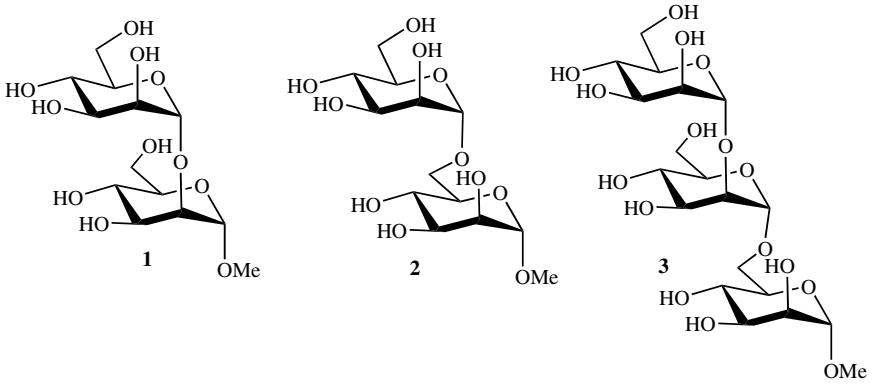

Figure 1. The oligosaccharides examined in this study.

GLYCAM_93 Molecular Dynamics (MD) simulations show that the linkage exists in two distinct, flexible conformations with similar ϕ value and different, slowly interconverting ψ values.[6] These results are consistent with X-ray data that show both conformations to be statistically represented.[1] The NOE contacts typically observed across the glycosidic linkage of α-Man-(1 → 2)-α-Man units are four (see below), and they are not consistent with any single conformation, suggesting either a highly flexible structure, or the presence of multiple conformers. The smallest range of conformers that would satisfy all the constraints is a range with ϕ ca. 60° and ψ spanning between −80° and −180°[1] (Fig. 1).

AMBER* calculations run on **1** with Macromodel 5.5 and using the GB/SA water solvation model are consistent with the GLYCAM results. The MC/EM conformational search shows two distinct minimum energy regions, which correspond to the 'stacked' (S, Fig. 2) and 'extended' (E, Fig. 2) conformations described by Woods et al.[6] The S region (ϕ 88°, $-90° \geqslant \psi \leqslant -58°$) displays a rather ample range of flexibility along ψ and contains the lowest energy conformation (ϕ, ψ 88°, −58°, Fig. 2c). Conformer E (ϕ, ψ 72°, −138°, Fig. 2d) is less stable than the former by 6 kJ mol^{-1}. Conformer S accounts for the NOE contact observed between H-1–H-1′ (Fig. 2, Table 1). Conformer E accounts for the H-5–H-1′ and H-1–H-3′ NOE contacts (Fig. 2, Table 1). The fourth observed NOE contact belongs to the interglycosidic H-1–H-2′ pair, which is at NOE distance in both conformations. Comparison of the calculated interproton distances with the experimental values[6] shows that the population of conformer S appears to be over-represented in the calculations. Two MC/SD dynamic simulations of **1** (5 ns each) starting from either S or E gave the same ϕ/ψ conformer distribution, suggestive of convergence rela-

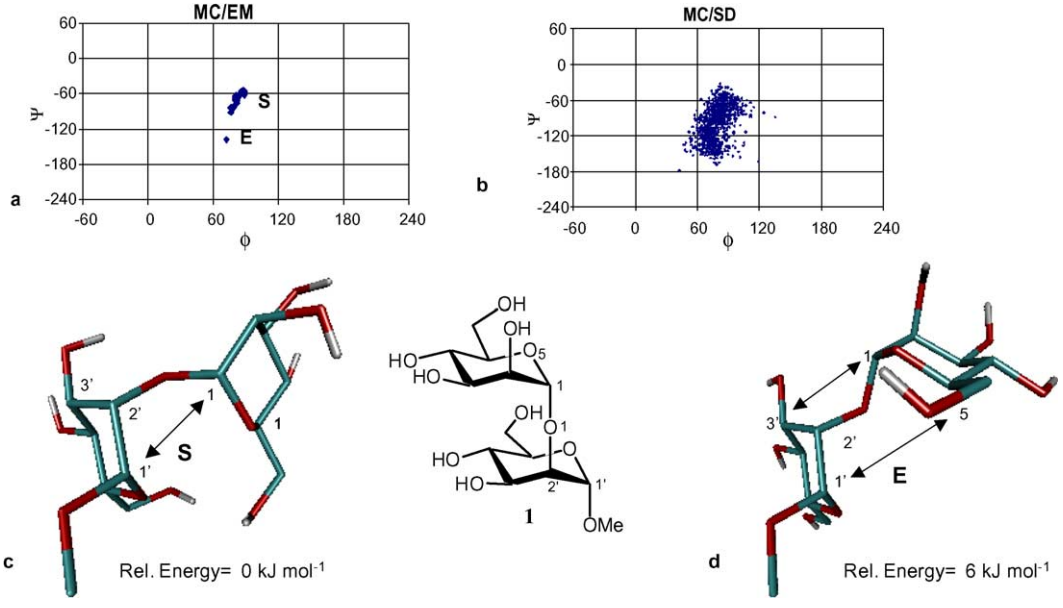

Figure 2. Conformational studies on α-(1 → 2)-mannobioside **1**. ϕ: O-5–C-1–O-1-C-2′; ψ: C-1–O-1–C-2′–C-1′. (a) 5000 steps of MC/EM conformational search; (b) 10 ns of MC/SD dynamic simulation; (c) the lowest energy, stacked conformation S (ϕ, ψ 88°, −58°); (d) the extended conformation E ($\Delta E = 6$ kJ mol^{-1}; ϕ, ψ 72°, −138°).

Table 1. Calculated interproton distances for **1**, **2**, and **3** (Å)

Linkage	Proton pair	1		2			3			Exp. range[d]
		MC/EM[a]	MC/SD[b]	MC/EM[a]	MC/SD[b]	MC/SD/EM[c]	MC/EM[a]	MC/SD[b]	MC/SD/EM[c]	
α(1→2)	H-1–H-1′	2.6	2.9		—		2.6	3.4	2.6	2.8–3.2
	H-1–H-2′	2.3	2.3		—		2.3	2.3	2.3	2.0–2.4
	H-1–H-3′	4.6	4.2		—		4.5	4.3	4.5	3.1–3.8
	H-5–H-1′	3.2	2.6		—		3.0	2.9	3.0	2.3–2.9
	H-1–H-4′	4.5	4.4		—		4.5	4.4	4.5	>3.5
α(1→6)	H-1–H-6a′		—	2.7	3.0	2.8	2.8	3.0	2.9	2.2–2.7
	H-1–H-6b′		—	2.5	2.5	2.5	2.5	2.5	2.5	2.0–2.3
	H-1–H-5′		—	3.0	4.0	3.0	2.7	3.9	2.6	—

[a]The distance is calculated from the Boltzmann weighted average, $\langle r^6 \rangle$, of the individual r_i^{-6} values found for conformations within 12 kJ mol^{-1} from the global minimum by the Monte Carlo search.
[b]Calculated from $\langle r^{-6} \rangle$ monitored during the simulation.
[c]Multiconformer minimization of the dynamic snapshots.
[d]Distance range from experimental data obtained for $Man_9GlcNAc_2$ from Ref. 6.

tive to these variables. The results, jointly reported in the torsional map of Figure 2b, show that the two conformers of the disaccharide interconvert rather freely, and are similarly populated. This description of the molecule is more compatible with the NMR data. Indeed, the agreement of the calculated average interproton distances and in particular of the critical NOE contacts H-1–H-1′ and H-5–H-1′ with the experimental value is improved, relative to the Monte Carlo results (Table 1, MC/SD column). Minimization of the conformations sampled during the simulation (Table 1, MC/SD/EM column) does not alter the position and relative energy of the minimum energy structures compared to the results obtained by the MC/EM search.

2.2. α-Man-(1→6)-α–Man-OMe (2)

The α-Man-(1→6)-α-Man linkage has been studied both by X-ray crystallography[1] and by NMR spectroscopy supported by molecular modeling.[6–12] All data give a constant ϕ value centered at ca. 60°, but they are somewhat at odds regarding the ω/ψ distribution. Statistic analysis of the X-ray data[1] shows that the linkage adopts three major conformations at ω/ψ *gt*/180° (28% of the available X-ray structures), *gt*/90° (28%), *gg*/180° (38%), and a minor one (6%) at *gg*/90°. NMR and molecular modeling data were obtained for the α-Man-(1→6)-α-Man-OMe disaccharide,[7–11] the α-Man-(1→3)-α-Man-(1→6)-β-Man-(1→4)-β-GlcNAc-1–OCD_3[12] tetrasaccharide, the α-Man-(1→3)-α-Man-(1→6)-α-Man-OMe trisaccharide,[8,9,11] and the α-Man-(1→6)-α-Man linkages in $Man_9GlcNAc_2$[6,10]. Analysis of the scalar coupling constants for the latter two structures suggests that the *gg* conformation is more populated than the *gt*.[6,8,11] For the α-Man-(1→6)-α-Man-OMe itself, the *gg*/*gt* ratio obtained by scalar coupling analysis is ca. 1:1.[7] The NOE analysis is generally not conclusive, because too few constraints are obtained. The results suggest two major conformations at *gt*/180° and *gg*/180°, but a ψ 90°,[6] or ψ 60°[8,9] conformation also appear to be transiently populated. Residual dipolar coupling constants have been measured for α-Man-(1→3)-α-Man-(1→6)-α-Man-OMe.[9] The results depend on the medium used, and indicate significant motion.

In our analysis, the MC/EM conformational search of **2** yielded 62 conformations within 12 kJ mol^{-1} from the global minimum. They all populate one state for ϕ, centered around 60° and two states for ψ, at 180° and 90°, the former being more stable than the latter. All the three ω rotamers were populated, and the first of the *tg* conformations was found to be just 1 kJ mol^{-1} above the global minimum. This result, which is contrast with experimental observations, is likely to be an effect of incomplete analysis of the hydrogen bond network (see below). Three 5 ns MC/SD simulations were run starting from the three lowest energy *gt*, *gg*, and *tg* conformers, respectively, yielding conformer populations, which differed by less than 2%. One thousand and five hundred snapshots were saved at regular intervals during each simulations, and they are reported in the ω, ψ plot of Figure 3. One major ω rotamer is clearly observed at 60° (*gt*, relative population 82%), followed by a minor one at −60° (*gg*, 12%). The *tg* region at ω 180° is barely populated (6%), as expected based on experiment. Thus, the low energy *tg* conformation found by the MC/EM search appears to be an artifact, likely due to incomplete sampling of the H bonding network distribution during the conformational search.

Further inspection of the *gt* population along the ψ coordinate reveals two clusters centered at ψ −180° (A_1, Fig. 3, 78% of the conformers) and 90° (A_2, Fig. 3, 22% of the conformers), whereas in the *gg* conformer the ψ torsion can freely oscillate between 90° and 180°. The results, therefore, are in qualitative agreement with Dwek's X-ray statistics,[1] but the calculation appears to

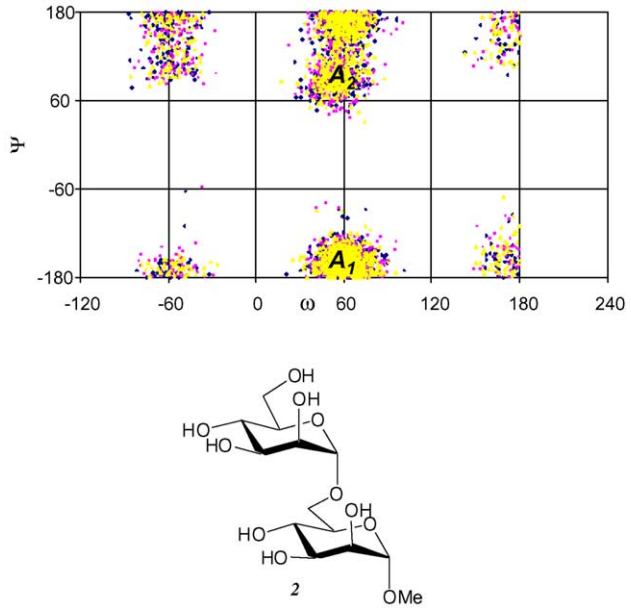

Figure 3. Conformational studies on the α-(1 → 6)-mannobioside **2** ω: O-1–C-6′–C-5′–O-5′; ψ: C-1–O-1–C-6′–C-5′. MC/SD simulations. The data reported in the ω/ψ plot were collected during three 5 ns simulations starting from one *gg* (blue series) one *gt* (purple series) and one *tg* (yellow series) initial conformations.

overestimate the population of the *gt* rotamer at the expenses of the *gg* one. The average, interproton distances observed during the simulation are compatible with the NMR data (Table 1).

Minimization of the conformers saved during the dynamic runs yielded 56 conformations within 12 kJ mol^{-1} from the global minimum, all lower in energy by ca. 8 kJ mol^{-1} than those found by the MC/EM search. The structures are collected in the ω/ψ plot of Figure 4. All the *tg* conformations are now relatively high in energy (relative energy $\geqslant$ 6.1 kJ mol^{-1}). The *gt* and *gg* conformations are clustered in four groups: A_1 at ω/ψ gt/−160°, A_2 at ω/ψ *gt*/90°, B_1 at ω/ψ *gg*/−160°, and B_2 at ω/ψ *gg*/100°. The lowest energy member of each cluster is reported in Figure 4, together with its relative energy. The interproton distances estimated by the Boltzman average over the MC/SD/EM minima are collected in Table 1.

2.3. α-Man-(1 → 2)-α-Man-(1 → 6)-α–Man-OMe (3)

This trisaccharide fragment is found as one of the 6-arms of the $Man_9GlcNAc_2$ oligosaccharide. Experimental data are available both from X-ray and NMR.[1,6] Adopting the same protocol used for the α-(1 → 6)-disaccharide, we generated initial conformations by a MC/EM search, and used them to run five separate 5 ns MC/SD dynamic runs. The starting conformations differed by the three ω, ψ_{1-6} and ψ_{1-2} coordinates, and were chosen so as to cover the conformational space available to the trisaccharide (see Section 4). The conformer population estimated by the five separate calculations differed by less than 5%. For both glycosidic linkages, the torsion angle ϕ was centered at 60° during the entire course of the simulation (20 ns, total). The conformations stored during one of the runs are collected in the $\omega/\psi_{1-6}/\psi_{1-2}$ torsion angle plot of Figure 5. The conformational map looks like the sum of the two maps obtained in the simulations of the (1 → 2) and (1 → 6) disaccharides (Figs. 2 and 3) and there appears to be no correlation between the motion of the two (1 → 2) and (1 → 6) glycosidic linkages. A continuum

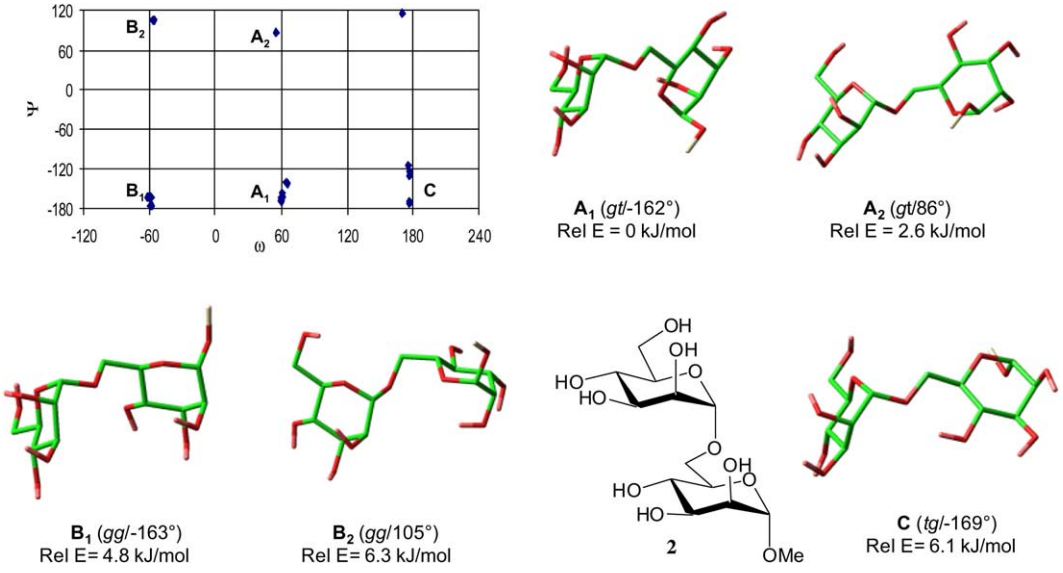

Figure 4. Conformational studies on the α-(1 → 6)-mannobioside **2** ω: O-1–C-6′–C-5′–O-5′; ψ: C-1–O-1–C-6′–C-5′. (a) Minimization of the structures stored during the dynamic simulation (MC/SD/EM). Conformations within 12 kJ mol^{-1} from the global minimum are shown in the ω/ψ plot. (b) The lowest energy conformation for each cluster is depicted, together with its relative energy.

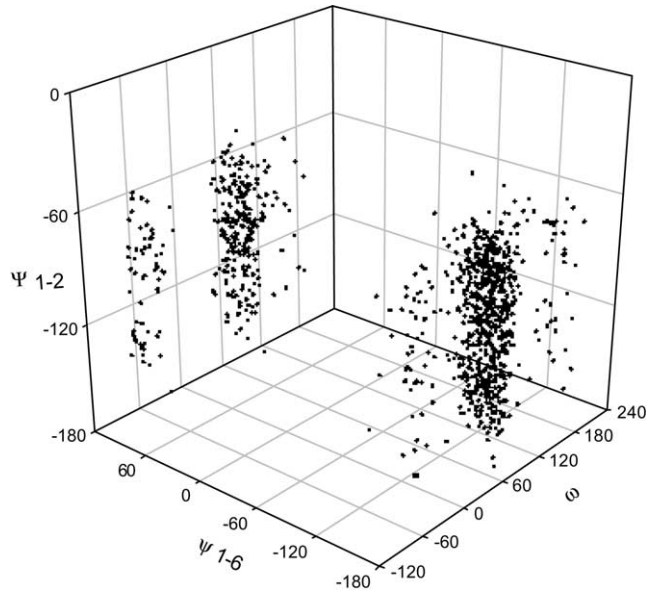

Figure 5. MC/SD simulation of **3**: ω, ψ_{1-6}/ψ_{1-2} torsion angles plots (ω: O-1–C-6′–C-5′–O-5′; ψ_{1-6}: C-1–O-1–C-6′–C-5′; ψ_{1-2}: C-1–O-1–C-2′–C-1′). The points represent conformations stored every 3.3 ps during the 5 ns dynamics.

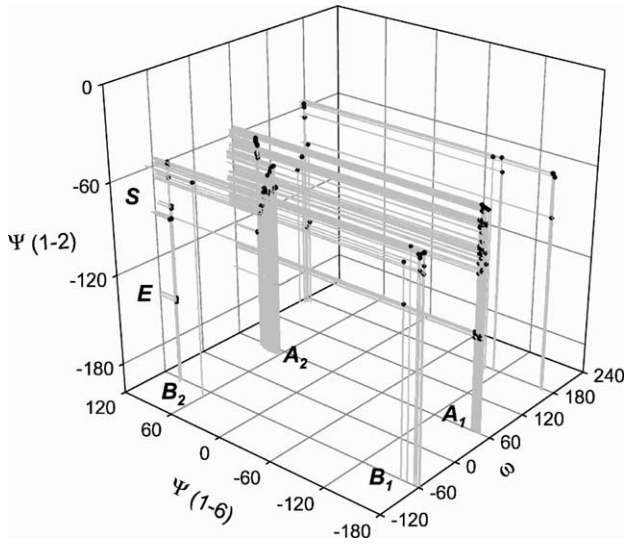

Figure 6. MC/SD/EM calculation of **3**: ω, ψ_{1-6}/ψ_{1-2} torsion angles plots (ω: O-1–C-6′–C-5′–O-5′; ψ_{1-6}: C-1–O-1–C-6′–C-5′; ψ_{1-2}: C-1–O-1–C-2′–C-1′) 7500 structures collected during five 5 ns dynamics were minimized. Minima within 12 kJ mol^{-1} from the lowest-energy one are collected in this picture.

motion takes from the stacked (S, ψ_{1-2} centered at −90°) to the extended (E, ψ_{1-2} −140°) conformation along the ψ_{1-2} torsion. The (1 → 6) linkage very briefly samples some *tg* conformations, but it is essentially represented by the four A_1 (ω/ψ_{1-2} *gt*/−160°), A_2 (ω/ψ_{1-2} *gt*/90°), B_1 (ω/ψ_{1-2} *gg*/−160°) and B_2 (ω/ψ_{1-2} *gg*/100°) conformations described for **2**. Energy minimization of the stored structures (MC/SD/EM) yielded 183 low-energy conformations within 12 kJ mol^{-1} from the global minimum. They are collected in the $\omega/\psi_{1-6}/\psi_{1-2}$ plot of Figure 6. Here some correlation is visible in that the (1 → 2)-extended conformation E is found as low energy only for the A_1 and B_2 clusters of (1 → 6)-linkage conformations, whereas it is not found within 12 kJ mol^{-1} for the (1 → 6)-B_1 and (1 → 6)-A_2 conformers. Therefore, based on this model, the α-Man-(1 → 2)-α-Man-(1 → 6)-α-Man-OMe trisaccharide **3** should be described as a combination of the six major conformations A_1S (ω, ψ_{1-6}/ψ_{1-2} 60°, −165°/−55°), A_2S (52°, 62°/−83°), B_1S (−58°, −180°/−56°), B_2E (−60°, 99°/−143°), B_2S (−56°, 105°/−55°), and A_1E (60°, −166°/−137°) depicted in Figure 7.

3. Discussion

The design of carbohydrate mimics has become an important field of study for the production of bioactive molecules.[13] Computational techniques can be used in this area, but they need to be validated with special care. Indeed, in the molecular design field, molecular modeling is essentially used to predict the structure of a yet nonexistent molecule and to compare it with the structure of the natural substrate to be mimicked. The first step of any design project, therefore, consists in a thorough evaluation of the three-dimensional shape of the natural effector based on computer modeling and on the use of available experimental data. As a second step, the same computational analysis is performed on the putative mimic, and its similarity to the natural template is evaluated, often on the basis of geometrical criteria. The use of techniques, which allow efficient sampling of the conformational space, is therefore essential in both these phases. With carbohydrates this task is particularly daunting, due the well-known flexibility of the structures and to the difficulties in obtaining experimental information. Traditional molecular dynamics techniques can give important information on the mobility of molecules, but they tend to sample conformational space very slowly. The MC/SD protocol, which mixes conformational leaps driven by the Monte Carlo steps with molecular dynamics exploration of local conformations, very efficiently yields a complete description of the conformational space available even to flexible and complex molecules, and thus appears to be particularly well suited as a computational tool for the study of carbohydrates.[3,4] We have extensively experimented with it on gangliosides[2] and ganglioside mimics,[14] and have found the method highly reliable when coupled with the AMBER* force field and the GB/SA water solvation model.

In this paper, we apply the technique to a small set of oligosaccharides of the oligomannose family, a group of oligosaccharides that have been heavily studied, and for which experimental data is copious.[1,6–12] The picture

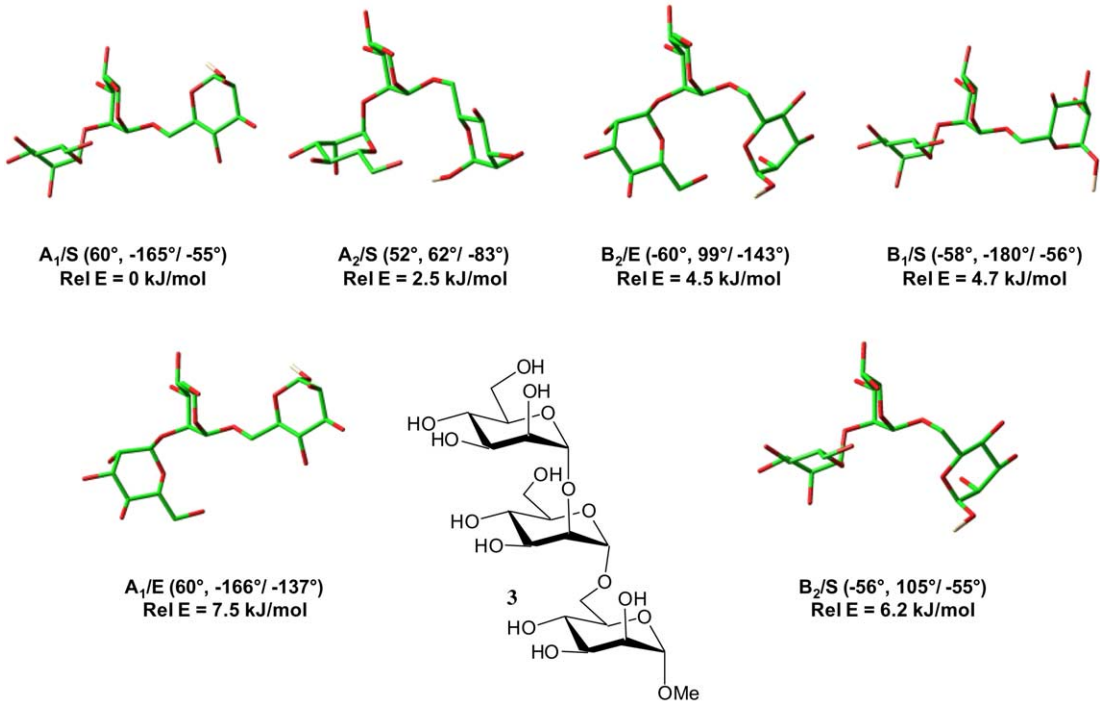

Figure 7. Conformational studies on the mannotrioside **3**. Low-energy conformations (12 kJ mol^{-1} from the global minimum) from the MC/SD/EM calculations. The lowest energy member of each cluster is shown. The data in parentheses are the values of the ω, ψ_{1-6}/ψ_{1-2} torsion angles (ω: O-1–C-6′–C-5′–O-5′; ψ_{1-6}: C-1–O-1–C-6′–C-5′; ψ_{1-2}: C-1–O-1–C-2′–C-1′).

obtained is in good agreement with the available information, and can be achieved with one simple set of calculations. Convergence of the MC/SD simulation is attained rapidly (5 ns simulations for the trisaccharide), as suggested by the analysis of multiple runs starting from different initial conformations.

The (1 → 6)-linked structures **2** and **3** represent a particularly demanding test. Computer modeling of (1 → 6)-glycosidic linkages has traditionally been difficult.[15] Weaknesses in the force fields and omission of the solvent effects combined with the slow convergence of traditional simulation methods all contribute to the difficulty of molecular dynamic calculations to generate conformational ensembles that display the correct rotamer populations for the ω torsion. Under our simulation conditions, the sampling problem is alleviated by the Monte Carlo steps in the MC/SD protocol, so that, at least for small molecules, the population ensembles are likely to reflect converged averages of the underlying energy surface. Using the AMBER* force field, MC/SD simulations in GB/SA water of reference monosaccharides show a tendency to overestimate the *gt* conformation at the expenses of the *gg* one.[†] This behavior is observed also in the present study. The experimental estimates of the *gt*/*gg* ratio in (1 → 6)-linked mannose disaccharides vary depending on the method used and the actual molecule studied, however, a prevalence of *gg* conformers,[6,9–11] or at best a 1:1 ratio of rotamers[1,7] is suggested in all circumstances. The AMBER*-GB/SA value of ca. 80:20 for the *gt*/*gg* ratio, therefore, appears to be biased toward the *gt* rotamer. It is nonetheless remarkable that a qualitatively adequate representation of the conformer distribution can be obtained from a single calculation (a 5 ns MC/SD dynamic simulation) even in this difficult case. Based on these findings, it appears that use of the protocol described in this paper is confirmed to be an appropriate tool for the computer-aided design of carbohydrate mimics. Work on developments of mannoside mimics is in progress in our group, and will be reported in due course.

4. Methods

All calculations were performed using the MacroModel/Batchmin[16] package (version 5.5) and the AMBER* force field with the Senderowitz–Still all-atom pyranose parameters.[17] Charges were taken from the force field (all-atom charge option). Water solvation was simulated using MacroModel's generalized Born GB/SA continuum solvent model.[5] This model treats the solvent as an

[†] For instance *gt*/*tg*/*gg* distributions of 77/13/10 and 60/34/6 were calculated by 1 ns simulations for 6-*O*Me-α-methylglucoside and 6-*O*Me-α-methylgalactoside, respectively. Estimated experimental values for glucosides and galactosides (from Ref. 15) are typically 40:0:60 and 50:35:15 (A. Bernardi, unpublished results).

analytical continuum starting near the van der Waals surface of the solute, and uses a dielectric constant of 78 for the bulk water and 1 for the molecule.

The conformational searches were carried out using 5000 steps for **1** and **2** and 15,000 steps for **3** of the usage directed MC/EM procedure. The interglycosidic linkages and the C-5–C-6 bonds were used as explicit variables during the Monte Carlo search. Extended nonbonded cutoff distances (a van der Waals cutoff of 8.0 Å and an electrostatic cutoff of 20.0 Å) were used. The interatomic distances r reported in Table 1 under the MC/EM header are calculated from the Boltzmann average of the r_i^{-6} of the individual conformations found by the search within 12 kJ mol^{-1} from the global minimum.

For the MC/SD[3,4] dynamic simulations van der Waals and electrostatic cutoffs of 25 Å, together with a hydrogen bond cutoff of 15 Å were used. This extension of the standard MacroModel/Batchmin values (8, 20, and 4 Å, respectively) slows the calculation, but allows for a smoother convergence, avoiding the strong energy increments that can arise from significant conformational changes. The dynamic simulations were run using the AMBER* all-atom force field. The same degrees of freedom of the MC/EM searches were used in the MC/SD runs. All simulations were performed at 300 K, with a dynamic timestep of 1.5 fs and a frictional coefficient of 0.1 ps^{-1}. Typically, runs of 5 ns each were performed, starting from conformations of the substrates, selected from the MC/EM outputs, which differed at glycosidic linkage. For **1** two initial conformations were used at ϕ, ψ 86°, −56°, and 72°, −137°, for **2** three conformations at ω/ψ *gt*/160° (A_1 in Fig. 4), *gg*/160° (B_1 in Fig. 4), and *tg*/170° (C in Fig. 4), for **3** five conformations at $\omega/\psi_{1-6}/\psi_{1-2}$ 61°/−167°/−58° (A_1-S), 55°/86°/−58° (A_2-S), −58°/−178°/−58° (B_1-S), 61°/−165°/−137° (A_1-E), 177°/−168°/−65° (C-S). The Monte Carlo acceptance ratio was about 4%, each accepted MC step was followed by an SD step. Structures were sampled every 3.3 ps and saved for later evaluation. Convergence was checked by monitoring both energetic and geometrical parameters. In general, when the simulations were stopped, the interproton distances and the conformer populations determined by each run differed by no more than 0.1 Å and 5%, respectively. The interatomic distances reported in Table 1 under the MC/SD header were evaluated from $\langle r^{-6} \rangle$ monitored during the simulation (option MDDI of Batchmin).

Minimization of the structures saved during the dynamic simulations was performed as a multiconformer minimization (MULT command of Batchmin), using the same energetic setup used in the MC/EM searches. The interatomic distances calculated from these sets of structures are reported in Table 1 under the MC/SD/EM header.

The glycosidic torsion angles are defined as follows: $(1 \rightarrow 2)$-linkage: $\varphi =$ O-5–C-1–O-1–C-2′, $\psi =$ C-1–O-1–C-2′–C-1′; $(1 \rightarrow 6)$-linkage: $\varphi =$ O-5–C-1–O-1–C-6′, $\psi =$ C-1–O-1–C-6′–C-5′, $\omega =$ O-1–C-6′–C-5′–O-5′.

Acknowledgements

This research has been supported by a Marie Curie Fellowship (to I.S.-M.) of the European Community programme IHP under contract number HPMT-CT-2001-00293, and by GlaxoSmithKline, Verona.

References

1. Wormald, M. R.; Petrescu, A. J.; Pao, Y.-L.; Glithero, A.; Elliot, T.; Dwek, R. A. *Chem. Rev.* **2002**, *102*, 371–386, and references cited therein.
2. Brocca, P.; Bernardi, A.; Raimondi, L.; Sonnino, S. *Glycoconj. J.* **2000**, *17*, 283–299.
3. Guarnieri, F.; Still, W. C. *J. Comput. Chem.* **1994**, *15*, 1302–1310.
4. Bernardi, A.; Raimondi, L.; Zanferrari, D. *J. Mol. Struct. (THEOCHEM)* **1997**, *395-396*, 361–373.
5. Still, W. C.; Tempzyk, A.; Hawley, R.; Hendrickson, T. *J. Am. Chem. Soc.* **1990**, *112*, 6127–6129.
6. Woods, R. J.; Pathiaseril, A.; Wormald, M. R.; Edge, C. J.; Dwek, R. A. *Eur. J. Biochem.* **1998**, *258*, 372–386.
7. Spronk, B. A.; Rivera-Sagredo, A.; Kamerling, J. P.; Vliegenthart, J. F. G. *Carbohydr. Res.* **1995**, *273*, 11–26.
8. Sayers, E. W.; Prestegard, J. H. *Biophys. J.* **2000**, *79*, 3313–3329, and references cited therein.
9. Tian, F.; Al-Hashimi, H. M.; Craighead, J. L.; Prestegard, J. H. *J. Am. Chem. Soc.* **2001**, *123*, 485–492.
10. Wooten, E. W.; Bazzo, R.; Edge, C. J.; Zamze, S.; Dwek, R. A.; Rademacher, T. W. *Eur. Biophys. J.* **1990**, *18*, 139–148.
11. Brisson, J.-R.; Carver, J. P. *Biochemistry* **1983**, *22*, 1362–1368.
12. Imberty, A.; Pérez, S.; Hricovini, M.; Shah, R. N.; Carver, J. P. *Int. J. Biol. Macromol.* **1993**, *15*, 17–23.
13. Sears, P.; Wong, C. H. *Angew. Chem., Int. Ed.* **1999**, *38*, 2300–2324, and references cited therein.
14. Bernardi, A.; Potenza, D.; Capelli, A. M.; García-Herrero, A.; Cañada, F. J.; Jiménez-Barbero, J. *Chem.—Eur. J.* **2002**, 4597–4612.
15. Kirschner, K. N.; Woods, R. J. *Proc. Natl. Acad. Sci. U.S.A.* **2001**, *98*, 10541–10545.
16. Mohamadi, F.; Richards, N. G. J.; Guida, W. C.; Liskamp, R.; Lipton, M.; Caufield, C.; Chang, G.; Hendrickson, T.; Still, W. C. *J. Comput. Chem.* **1990**, *11*, 440–467.
17. Senderowitz, H.; Still, W. C. *J. Org. Chem.* **1997**, *62*, 1427–1438.